ELSEVIER

Polymer 40 (1999) 3331–3344

polymer

Poly(methacrylic acid)–copper ion interactions Phase diagrams: light and X-ray scattering

Caroline Heitz, Jeanne François*

Laboratoire de Recherche sur les Matériaux Polymères, Uniiversité de Pau et des Pays de l'Adour, CNRS, Helioparc. 2 Avenue du Président Angot, 64 000 Pau, France

Received 28 October 1997; received in revised form 12 January 1998; accepted 23 January 1998

Abstract

The interaction of a sample of poly(methacrylic acid) with copper ions is investigated using various techniques: light and X-ray scattering, viscosimetry and fluorescence. The measurements were performed in the solubility domains and the regions where phase separation occurs were determined as a function of pH and copper/polymer ratio. We conclude that copper is mainly bound on the polymer through the formation of binuclear complexes implying pairs of adjacent carboxylates far along the chain. This induces a strong collapse of the chain at low ionisation degree and partially hinders the chain expansion at high pH. Fluorescence measurements can be interpreted through the existence of two different transitions: local and global transitions.

Keywords: Poly(methyacrylic acid); Interactions with copper ions; Chain conformation

1. Introduction

Despite a great number of works dealing with poly (methacrylic acid) (PMA), many uncertainties remain regarding its behaviour in aqueous solution. This may be due to its ability to adopt a compact structure at low ionisation degree, α, and to undergo a conformational transition in the range $0.15 < \alpha < 0.4$ [1–6]. This is reflected by unusual variations of the pK_a and of the reduced viscosity versus α. We have recently undertaken a systematic study of the behaviour of PMA in water in the absence and in the presence of divalent cations, using a PMA sample of relatively low molecular weight. We have carried out a series of light and X-ray scattering investigations in pure water or with added NaCl and shown that the existence of helicoidal portions in the compact structure may account rather well for the behaviour in the high scattering vector range [7,8]. When ionisation increases, the scattering function is characterised by a correlation peak, with a discontinuous variation of the maximum position q^* versus α as a manifestation of the conformational transition.

On the other hand, one of the most interesting features of polyelectrolytes is their capacity to bind counterions and particularly multivalent cations [9–16]. This property is extensively used, for example, in depollution processes. However, if the behaviour of polyelectrolytes in pure water or in the presence of simple salts is relatively well understood [17–27], the phase separation, the nature of the interactions and the conformational changes in the presence of multivalent cations have been until now the object of only a small number of reliable investigations. However, some studies of the interactions between PMA and copper ions were made in the 1960s, particularly by the Mandel and Leyte group who used methods such as potentiometry, viscosimetry, u.v.–vis spectroscopy and dialysis equilibrium [28–30]. These authors have clearly demonstrated the formation of complexes between Cu^{2+} and the PMA carboxylates. The u.v.–vis behaviour was interpreted in terms of the formation of a binuclear complex implying four COO^- per two Cu^{2+}, at low pH and by a mononuclear complex of the type $Cu(COO)_2$ at higher pH. A recent electron paramagnetic resonance of the PMA–copper interactions lead us [31] to propose a description different from that of Mandel and Leyte [28,29]. We concluded that the binuclear complex is predominant in the whole range of pH. The question arises from the possible conformation of the PMA chain compatible with the formation of such binuclear complexes. We have also shown that for polyelectrolytes of lower density of carboxylates, (partially hydrolysed polyacrylamide (PAAM)) the mononuclear complex is favoured. This means that the formation of binuclear complexes requires a high density of ionisable groups. Moreover, the presence of carboxylate sequences seems to favour the binuclear complexes, if the polymers are compared at

* Corresponding author.

0032-3861/99/$ - see front matter
PII: S0032-3861(98)00126-8

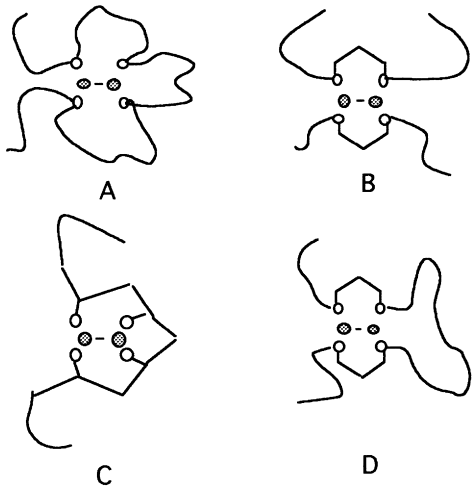

Fig. 1. Schemes of the possible structures of the binuclear complexes PMA/copper.

the same charge density. The several possible schemes for a PMA chain in interaction with copper ions are presented in Fig. 1. The first one (A) where four carboxylates are randomly distributed along the same chain can be eliminated through the above observations. Case (C) where four adjacent groups are involved in the complex seems improbable due to the chain rigidity. If two pairs of adjacent groups belonging to different chains are assumed to form the complex, aggregation is expected, which should be detected by light scattering. Finally, model (D), where the complexation is a intramolecular phenomenon and implies pairs of adjacent groups, is associated to a chain folding and to a collapse of the macromolecular coil without aggregation. The aim of the present work is to give some further information on the PMA conformation in the presence of copper ions through investigations using various techniques (light and X-ray scattering; viscosimetry, fluorometry). In the next section, we will discuss the phase diagrams established in order to perform the scattering investigations only in the range of solubility. Moreover, some experiments will be performed in the presence of other cations for comparison.

2. Experimental

2.1. Polymer sample

The polymer sample was prepared by radical polymerisation, as described in previous works [7,8]. It was characterised by size exclusion chromatography, using mono- and multi-angle light scattering detection. Its molecular weight is 56 000 ± 2000 and its polydispersity index is close to 2.

2.2. Experimental methods

2.2.1. Phase diagrams

Solutions of copper chloride or (nitrate) and PMA were prepared separately and gently stirred for 24 h up to complete solubilisation Two equal volumes of these solutions were mixed in several tubes. Then aliquots of an NaOH solution were added to adjust the pH at different values in the tubes. The mixtures were then vigorously stirred and kept at rest at room temperature for 48 h. Then visual observations were made and the pH was measured.

2.2.2. Fluorescence

This technique is well adapted to the characterisation of micelles or hydrophobic microdomains in the amphiphilic systems [32,33]. One generally uses a hydrophobic probe whose vibronic properties depend on the polarity of its neighbouring environment. For instance, in the case of pyrene, which we used in this study, the ratio of the intensity of the first to the third peaks of its emission spectrum is equal to 1.9 in water and 0.6 in cyclohexane.

The solutions of PMA–copper were prepared as described for the phase diagrams, but the solvent was pyrene saturated water (5×10^{-7} mol l^{-1}). The measurements were made with a Hitachi F4010 spectrofluorometer. The excitation wavelength was set to 335 nm.

2.2.3. Static light scattering

The static light scattering measurements were carried out with two different types of apparatus:

- a commercial one (SEMATECH) equipped with a He–Ne laser source (wavelength $\lambda = 632$ nm);
- a home-built one equipped with an Ar laser source ($\lambda =$ 514 nm) [34].

The scattering angle θ was varied between 30 and 150°.

2.2.3.1. Preparation of the solutions. First a mixture of PMA in its acid form and copper salt was prepared and solubilised. Different solutions at various pH values were then prepared by addition of small amounts of a filtered NaOH solution. The partially neutralised solutions were filtered on 0.2 μm membranes (Dynagard) directly in the measurement cells.

2.2.3.2. Determination of the refractive index increments dn/dc. As the copper ions are expected to bind on the polymer, it is necessary to measure the dn/dc for these solutions after dialysis equilibrium. On the other hand, the copper complexation induces a strong absorption in the visible range and a dn/dc increase in this wavelength domain. The dn/dc measurements must be made at exactly the same λ as that used for light scattering measurements.

A Brice–Phoenix refractometer was used for the measurements at 488 nm. The experimental conditions were polymer concentration $C_p = 2.06 \times 10^{-3}$ g ml^{-1}, copper concentration C_{Cu}=3 mM, NaCl concentration $C_{NaCl} = 0.05$ M. The following variation of dn/dc versus the ionisation degree α was found to be:

$$\frac{dn}{dc} = 0.168 + 0.1056 \times \alpha \ (\text{ml g}^{-1}) \quad (1)$$

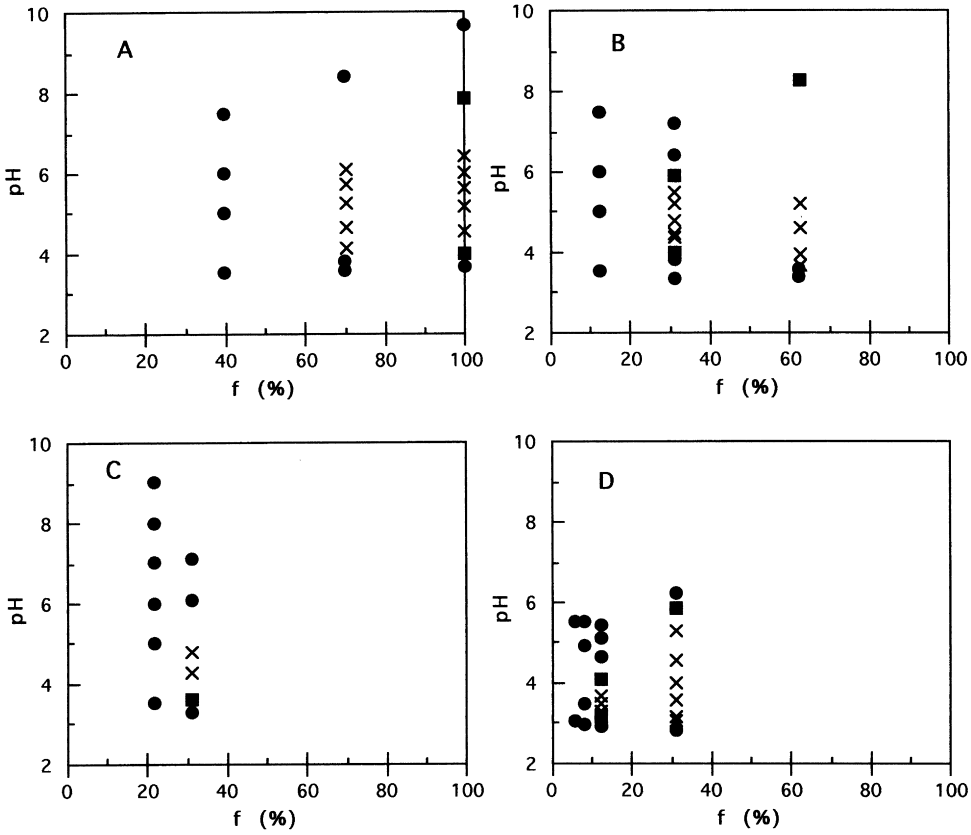

Fig. 2. Phase diagrams of the system PMA–copper in water: homogeneous solution (●), phase separation (×). (A) $C_p = 2.5$ mM; (B) $C_p = 8$ mM; (C) $C_p = 16$ mM; (D) $C_p = 100$ mM.

2.2.4. Dynamic light scattering

We used a dynamic light scattering apparatus constructed in our laboratory by Duval [35]. It is equipped with an Ar laser of 5 W. The wavelength was set at 488 nm. The scattered intensity is measured by a photomultiplier Hamatsu. The correlation function is obtained using an ALV 3000 correlator of 192 channels in the 'multitau' mode. The 'CONTIN' method was used to determine the distribution of the relaxation times, $G(\Gamma)$:

$$\left|g^{(I)}(q,\tau)\right| = \sum_0^\infty G(\Gamma)\mathrm{e}^{-\Gamma\tau}\,\mathrm{d}\Gamma \tag{2}$$

where q is the scattering vector. The measurements were made at $\theta = 90°$.

2.2.5. Small angle X-ray scattering

The small angle X-ray scattering (SAXS) experiments were made at the LURE laboratory using the D24 apparatus. We used a wavelength $\lambda = 1.488$ Å and the sample–detector distance was set at 2.003 m. The transmission measurements were made with a carbon black sheet introduced between the sample and the detector, for a short time before and after the registration of the intensity scattered by the sample.

The total scattered intensity $I_{tot}(i)$ for the channel i, normalised to the incident intensity is given by:

$$I_{tot}(i) = I_{sam}(i) \times Tr(\mathrm{CB}) + I_{CB}(i) \times Tr(\mathrm{sam}) \tag{3}$$

where I_{sam} and I_{CB} are the intensities scattered by the sample alone and the carbon black alone respectively. Tr(sam) and Tr(CB) are their transmissions. That of the sample Tr(sam) can be obtained from the following expression:

$$Tr(\mathrm{sam}) = \frac{\sum_i I_{tot}(i) - Tr(\mathrm{CB}) \times \sum_i I_{sam}(i)}{\sum_i I_{CB}(i)} \tag{4}$$

In this expression, the term $Tr(\mathrm{CB}) \times I_{sam}(i)$ is much lower than I_{tot}. Finally, the excess of scattered intensity with respect to the solvent is given by:

$$I = \left(\frac{I_{sam}(i)}{Tr(\mathrm{sam})} - \frac{I_{ec}(i)}{Tr(\mathrm{ec})}\right) - \Phi_v^{sol}\left(\frac{I_{sol}(i)}{Tr(\mathrm{sol})} - \frac{I_{ec}(i)}{Tr(\mathrm{ec})}\right) \tag{5}$$

where the 'ec' index corresponds to the empty cell and the 'sol' index corresponds to the cell filled with the solvent and Φ_v^{sol} is the volume fraction of the solvent.

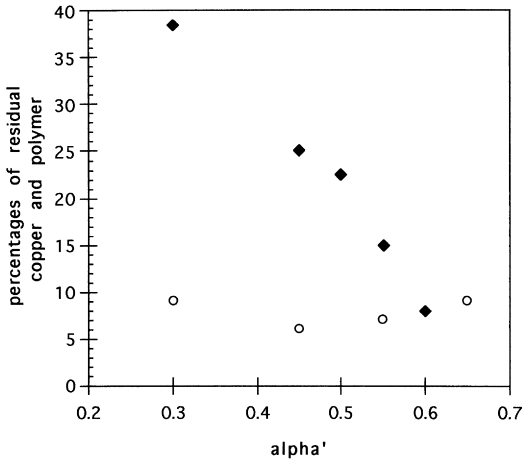

Fig. 3. Phase diagrams: concentrations of copper (◆) and polymer (○) in the supernatant phase.

3. Results

3.1. Phase diagrams

3.1.1. Experimental results

Fig. 2A–D give the phase diagrams where the abscissa is the stoichiometric ratio $f = C_{Cu}/C_p$ and the ordinate is the pH. C_{Cu} is the molar concentration of copper ions and C_p is the molar concentration of PMA monomer units.

At a given concentration, C_p, and for f lower than a value f_s, the system is homogeneous in the whole range of pH. For $f > f_s$, a phase separation is observed in an intermediate range of pH, this region increases with increasing the f value.

When the polymer concentration increases, the phase separation region becomes more and more important and the value of f_s decreases.

The amount of copper and polymer contained in the homogeneous supernatant were determined through u.v.–vis spectroscopy and organic carbon measurements respectively. These amounts normalised to those initially contained in the mixtures are plotted in Fig. 3 as a function of the degree of neutralisation of the polymer. The polymer percentage passes through a minimum at $\alpha' = 0.45$ and is always lower than 10. In the same range of α', the copper amount continuously decreases. From these values, it is possible to calculate the composition of the precipitated phase in terms of the total number of carboxylates ([COOH] + [COO^-]) per copper atom (X_A) or of the number of ionised groups ([COO^-]) per copper atom (X_B). We assume:

$$[COO^-] = \alpha([COOH] + [COO^-]) \quad (6)$$

The results are reported in Table 1. Moreover, we have registered u.v. absorption spectra of the supernatant phase. Their characteristics are those of free copper and it seems that the copper present in this phase is not 'complexated' by the polymer. This suggests that the residual organic carbon contained in this phase is not due to polymer residues but to organic impurities. Finally, the copper concentration decreases continuously with α' up to its total binding while the solution phase separates when a given fraction of the carboxylates is neutralised by the copper ions. If we extrapolate the X_A values at the α' value corresponding to the onset of the phase separation, $X_A = 5.4$, the polymer becomes insoluble when 17% of the carboxylates are bound to a copper ion.

Table 1
Results of the determination of the contents of polymer and copper in the supernatant

α'	Total number of carboxylates in the precipitated phase	Number of copper ions in the precipitate	X_A	X_B
0.3, pH = 4.2	7.3×10^{-3}	1.543×10^{-3}	4.74	1.42
0.45, pH = 4.5	7.56×10^{-3}	1.86×10^{-3}	4.04	1.83
0.55, pH = 4.6	7.51×10^{-3}	2.12×10^{-3}	3.85	1.94
0.6, pH = 4.9	7.37×10^{-3}	2.293×10^{-3}	3.46	1.93

3.1.2. Interpretation

These phase diagrams can be qualitatively well understood from the different approaches which have been developed in order to predict the behaviour of polyelectrolytes in the presence of multivalent ions [36–38].

It is generally assumed that the system is ruled out by a series of equilibria.

1. The hydrolysis of the ions

   $$xM^{2+} + yH_2O \rightarrow M_x(OH)_y^{2x-y} + yH^+$$

   with associated formation constants

   $$K_{xy} = \frac{[M_x(OH)_y^{2x-y}][H^+]^y}{[M^{2+}]^x} \quad (7)$$

   for a divalent ion such as copper.
2. (ii) The acid–base equilibrium of the carboxylates with the constant:

   $$K_a = \frac{[COO^-][H^+]}{[COOH]} \quad (8)$$

3. (iii) The formation equilibrium of the mono- and binuclear complexes where respectively two carboxylates and one copper atom (COO_2Cu) or four carboxylates and two copper atoms (COO_4Cu_2) are involved. There are many controversies on the existence and formation of these complexes according to the nature and the degree of neutralisation of the polyacid. The first work of Leyte et al. [30] lead to the conclusion that the binuclear complex is formed at low pH and disappears at higher pH where the mononuclear one is preponderant. In a more recent spectroscopic study we have compared EPR and u.v.–vis results and shown that this model

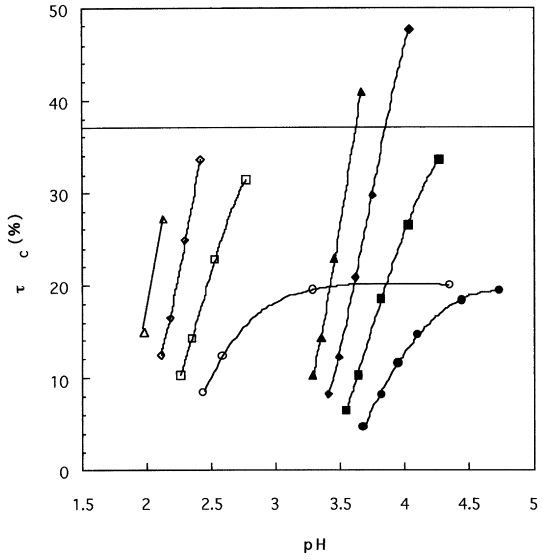

Fig. 4. Calculated fraction of 'complexated' units as a function of pH. $C_{pM} = 8$ mM; $f = 0.1$ (●), $f = 0.2$, (■), $f = 0.4$, (◆), $f = 0.6$ (▲). $C_{pM} = 100$ mM; $f = 0.1$ (○), $f = 0.2$, (□), $f = 0.4$, (◇), $f = 0.6$ (△).

can be successfully applied to the cases of polyacrylic acid, while for PMA mainly binuclear complexes are formed in the whole range of pH [31]. Then, our experimental results could be quantitatively adjusted by considering the following equilibrium:

$$4COO^- + 2Cu \rightarrow COO_4Cu_2$$

with the constant K_{pCu}:

4.

$$K_{pCu} = \frac{[COO_4Cu_2]}{[COO^-]^4[Cu^{2+}]^2} \quad (9)$$

By combining these different equilibrium equations (Eqs. (7)–(9)), it is easy to resolve the system and obtain the concentration of each species. The results were in good agreement with the EPR results, using $K_{pCu} = 10^{17}\,l^4\,mol^{-4}$.

In contrast, the solubility of the polymer is related to the fraction of carboxylates which are respectively under the acid form (A), the ionised form (B) or the complexated form (C). Clearly, the more ionised the polymer, the higher its solubility in water and, inversely, the higher the number of groups forming a binuclear complex with copper, the lower the solubility. Then, it has been proposed to write the free energy of the system as the sum of three terms corresponding to the three carboxylic forms, using the classical Flory formulations.

$$\frac{F}{kT} = \frac{F_A}{kT} + \frac{F_B}{kT} + \frac{F_C}{kT} \quad (10)$$

where:

$$\frac{F_A}{kT} = \frac{1}{2}\nu_A(\tau_A)^2C_p^2 + \frac{1}{3}\omega_A^2(\tau_A)^3C_p^3 \quad (11)$$

$$\frac{F_B}{kT} \cong \frac{1}{2N_aI}(\tau_B)^2C_p^2 \quad (12)$$

$$\frac{F_C}{kT} = \frac{1}{2}\omega_C(\tau_C)^2C_p^2\frac{F_C}{kT} \cong \frac{1}{2}\nu_C(\tau_C)^2C_p^2 \quad (13)$$

- τ_A, τ_B and τ_C are the fractions of carboxylates under their form A, B and C respectively;
- ν_A and ω_A are the excluded volume parameters and the third virial coefficient associated to the A form; They are positive;
- I is the ionic strength of the solution;
- ν_C is the excluded volume parameter associated to the C form. It is assumed to be strongly negative.

The phase separation is expected to occur when:

$$\frac{\partial^2 F}{\partial C_p^2} = 0 \quad (14)$$

and

$$\nu_A\tau_A^2 + \frac{\tau_B^2}{N_aI} + \nu_C\tau_c^2 = 0 \quad (15)$$

In the presence of multivalent cations and in the absence of salt the ionic strength can be simply considered as equal to $I = C_B\tau_B$ and relation (15) becomes:

$$\nu_A\tau_A^2 + \frac{\tau_B}{N_aC_p} + \nu_C\tau_C^2 = 0 \quad (16)$$

This condition can be realised as well at low pH, when the polymer is weakly charged and the fraction of units C high enough (precipitation) as at higher pH when the ionisation of the carboxylates becomes sufficient to provoke the resolubilisation.

3.1.2.1. Precipitation at low pH

- At $\alpha' = 0$, the fractions of the A and C units are low, then the second term of Eq. (16) is close to zero while the absolute value of the third term remains lower than that of the first one. Then, the polymer is soluble.
- When α' increases, the polymer binds more and more copper and two situations can be considered:

1. The complexation constant K_{pCu} is very high and only units A and C are present in the system. In other terms, the acid–base equilibrium is completely shifted by the presence of the copper ions. The second term can be neglected and the phase separation should occur when:

$$-\frac{\tau_C^2}{(1-\tau_C)^2} = \frac{\tau_A}{\tau_C} \quad (17)$$

for a fraction of C units independent of the polymer concentration.

2. K_{pCu} is not high enough to hinder the formation of

ionised carboxylates. One can then predict that the lower the C_p, the higher the fraction τ_C required for the phase separation. Our experimental results illustrate such a situation. An attempt to make our analysis more quantitative can be made, using the values of the constants previously obtained [31] and assuming that K_a is constant (at $\alpha' = 0$, $4.90 < pK_a < 5.67$, when C_p varies between 0.57 and 0.0084 M l^{-1} for solutions of pure PMA. Fig. 4 gives the calculated fractions of the units C versus pH for two polymer concentrations and several values of the f parameter. As expected, at a given pH, τ_C increases when f and C_{pM} increase. For the lower polymer concentration, $C_{pM} = 8$ mM, we have observed that phase separation occurs at a pH corresponding to $X_A = 5.4$ and to a critical value $\tau_C^* = 0.37$ for $f = 0.31$. Let us assume that this fraction τ_C^* is that required for phase separation at this concentration of polymer; it is represented by the horizontal line in Fig. 3. This figure shows very well that for f lower than approximately 0.18, the value τ_C^* cannot be reached and then the polymer remains soluble, while for higher values of f, τ_C^* is obtained for a pH value which decreases when f increases, in agreement with the experimental observations. At a higher polymer concentration, if the τ_C^* value is the same, it is quite clear that phase separation should occur at much lower pH, as observed. In fact, we expect a lower value of τ_C^* due to the lower ionisation and the real shift must be higher.

3.1.2.2. Re-dissolution at high pH. When α' increases after the total binding of the copper ions present in the solution, one has also to consider two situations.

1. $f < 0.5$, then $\tau_C = 2f$ and the re-dissolution is expected when:

$$\nu_A(1 - 2f - \tau_B)^2 + \frac{\tau_B}{N_a C_p} + (2f)^2 \nu_C = 0 \qquad (18)$$

The first term can be neglected since the fraction of COOH units becomes very low and the associated virial much lower than the electrostatic virial of the charged units B. This expression shows that the fraction of B units must increase when f increases, in agreement with the experimental observations. Nevertheless, it is difficult to approach this limit more quantitatively, because the variation of the K_a with the polymer ionisation and the polymer conformation must be taken into account.

2. $f > 0.5$, all the carboxylates are theoretically involved in the formation of a complex and in our approach, no re-dissolution is expected since only units of low virial will be present on the polymer. In fact, this phenomenon is observed and one of the possible explanations is the competition of the complexation and hydrolysis equilibrium of copper. We have indeed observed that in such a case the nature of the precipitate changes and that it contains less polymer than expected.

In conclusion to this phase diagram study, it appears that the solubility limits can roughly be understood through a simple thermodynamic model, by considering that copper and carboxylates form binuclear complexes insoluble in water. The solubility results mainly from an excess of charged groups at high pH and an excess of acid groups at low pH. The results are in agreement with the previous investigations using e.p.r. to quantitatively determine the percentages of the different units.

3.2. Light scattering experiments

3.2.1. Static light scattering

Let us recall that the PMA sample used in this study has a relatively small molecular weight and consequently a small radius of gyration R_g ($R_g = 50$ Å for $\alpha = 0$ [7,8]). In the light scattering experiments performed in the absence of salt, no angular dependence of the scattered intensity was observed since $qR_g \ll 1$. In the presence of copper the formation of aggregates due to intermolecular complexation could be expected with an excess of scattered intensity at small angles. All the experiments were performed at low polymer concentration corresponding to the dilute regime in the absence of copper, according to the evaluation of the critical overlap concentration through viscosity measurements [8]. Moreover, the ratio f was chosen so that the polymer remains soluble (see phase diagrams). We have considered two cases: in the presence and in the absence of added salt (NaCl).

(a) In the presence of NaCl (0.05 M), we used two polymer concentrations $C_p = 2.06 \times 10^{-3}$ g ml^{-1} and 0.68×10^{-3} g ml^{-1} corresponding to $C_{pM} = 24$ mM and 8 mM respectively, and to a ratio $f = 0.125$ in both cases. The value of α' was varied by addition of NaOH. The scattered intensity was never dependent on the scattering angle, which demonstrates the absence of aggregates in our experimental conditions. We can deduce that for low enough polymer concentrations, in the dilute regime and in the presence of salt, the formation of binuclear complexes is only an intramolecular phenomenon. We have also observed that the variations of I/KC_p versus α' do not differ significantly from that observed in the absence of copper (K is the optical constant and I the excess of scattered intensity of the solution with the respect to the solvent).

(b) In the absence of salt, we used the same concentration as for X-ray scattering: $C_p = 9 \times 10^{-3}$ g ml^{-1}. No excess of scattered intensity was observed, meaning that even in pure water no aggregates are formed and we will discuss only results obtained at $\Theta = 90°$. One can compare in Fig. 5 the variations of I/KC_p versus C_p obtained at $\alpha' = 0$: (i) in the presence copper ($f = 0.125$), (ii) in the absence of copper, (iii) with addition of 0.1 M HCl (in order the eliminate the self-ionisation of the polymer). The values of I/KC_p are much higher in the presence of copper than in pure water

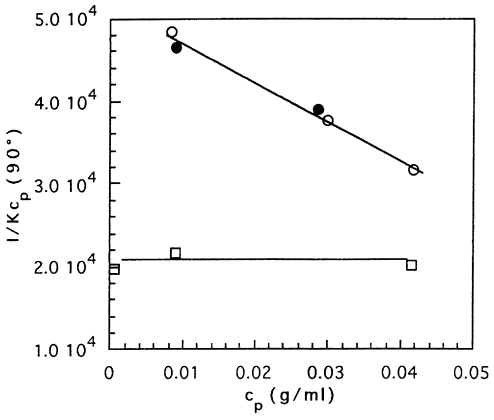

Fig. 5. Static light scattering: variations of I/KC_p (90°) versus C_p at $\alpha' = 0$: in the presence of copper ($f = 0.125$) (●) in pure water (□), in 0.1 M HCl (○).

and almost equal to those obtained in 0.1 M HCl, at zero ionisation. This behaviour can have two origins, the complete binding of copper which leads to the formation of a neutral polymer or, more probably, a screening out of the electrostatic repulsions by the excess of non-bound copper ions. When the degree of neutralisation increases, I/KC_p decreases as in pure water (see Fig. 6) but the values obtained in the presence of copper are higher. This can be qualitatively due to the copper binding which reduces the polyelectrolyte effect. It can be shown that for $\alpha' > 0$ the discrepancies between the two curves are reduced if this binding is taken into account (the true ionisation degree is calculated using the complexation constants) which leads to a decrease in the value of α' when copper is present.

3.2.2. Quasi-elastic light scattering

Fig. 7a shows examples of diffusion coefficient distributions obtained with PMA solutions ($C_{pM} = 24$ mM) in the presence of copper ($f = 0.125$) and salt (NaCl 0.05 M) and for various values of α'. These distributions are always monomodal and their broadening when α' increases is negligible. The average diffusion coefficient D seems to be constant up to the total copper binding represented by the vertical line on Fig. 7b and then it decreases. The same evolution was observed by viscosimetry (see below). The hydrodynamic radius of the macromolecules (deduced from D using the classical Stokes–Einstein relation) is approximately 49 Å during the binding step and when an excess of charged carboxylates appears, it increases and tends toward 60 Å for $\alpha' = 0.9$. Under the same conditions but in the absence of copper, D is generally lower, in agreement with a higher average charge density.

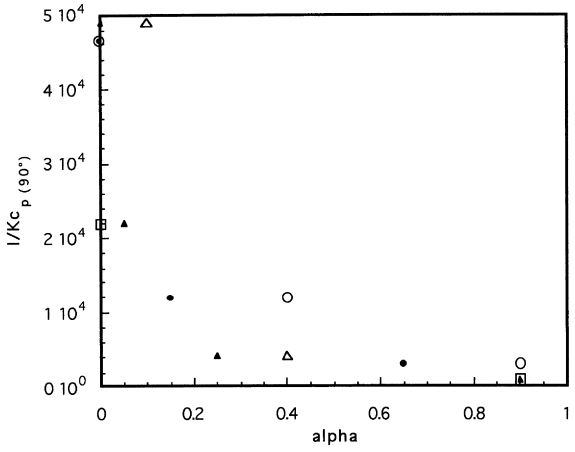

Fig. 6. Static light scattering: variations of I/KC_p (90°) as a function of the degree of neutralisation α' (open symbols) or of the true degree of ionisation (filled symbols) in pure water (□,■), in the presence of copper $f = 0.08$ (▲,△), $f = 0.125$ (●,○).

In the absence of copper and salt, it is difficult to make significant measurements, due to very low scattered intensity. When copper is added to solutions, the results become better and some results are given in Table 2. In all the cases, the distribution of D is monomodal. For $\alpha' = 0$ and at a given C_p, D is lower in the presence of copper than in pure water. In this last case, a coupling with the free counter ions tends to increase the value of D, while this effect is reduced by the copper binding. Generally D increases when α' increases, in opposition to the behaviour observed in the presence of NaCl. We have shown that PMA in pure water is characterised by a bimodal distribution of D with a fast mode corresponding to a D_f value approximately seven times higher than that of the slow mode, D_s. Sedlak et al. [39] have observed an increase of D_f with increasing α'. Finally, the behaviour in the presence of copper is that of a polyelectrolyte, the effects being attenuated by the binding phenomenon. It is clear that under these conditions of concentration no aggregates are formed due to the copper PMA interactions. This suggests that model D (Fig. 1) is the more appropriate to give a good account of both the structural and spectroscopic observations.

3.3. X-ray scattering

3.3.1. Results

The structure of PMA solutions containing divalent cations has never been investigated, to the best of our knowledge. It was interesting to compare the scattering functions of this system with those obtained with a monovalent cation Na^+ and another divalent one, Ni^{2+}, which is known to interact less strongly with polycarboxylates. The aim of this comparison is to clearly differentiate the effects due to complexation from those related to the electrostatic screening out.

In all these X-ray experiments, we kept the polymer concentration constant, $C_p = 9 \times 10^{-3}$ g ml^{-1}, the salt concentrations were 8.35 mM for copper nitrate and nickel sulphate ($f = 0.125$) and 0.025 M for sodium nitrate. The total binding of copper occurs at $\alpha' = 0.16$. The evolution of the scattering curves as a function of α' for PMA in pure water and for the three salts can be compared in Figs. 8′

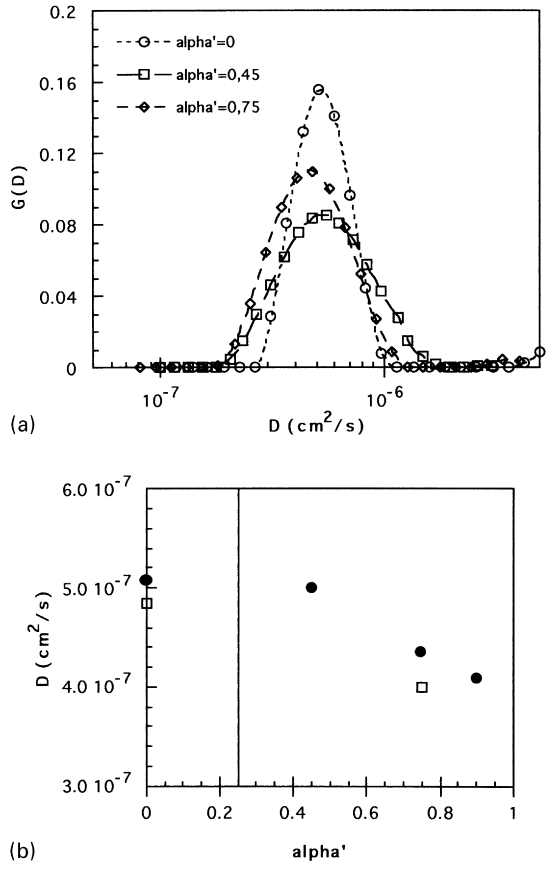

Fig. 7. Dynamic light scattering. (a) Evolution of the distribution function $G(D)$ as a function of α', $C_{pM} = 24$ mM ($C_p = 2.06 \times 10^{-3}$ g ml^{-1}) and $C_{Cu} = 3$ mM ($f = 0.125$) (the lines are guides for eyes). (b) Variation of D with α' in pure water (□) in the presence of copper (●).

increases, while generally the intensity at this maximum I_{max} continuously decreases. The case of PMA is more complicated due to the conformational change which occurs at $0.15 < \alpha' < 0.35$, as shown in previous studies [31,39]. Moreover, when X-rays are used, several authors have shown that I_{max} passes through a minimum. Heitz et al. [31] explained such a behaviour, taking into account the ionic condensation when $\alpha' > 0.5$. In the small q range, the scattered intensity generally decreases when α'

Table 2
Diffusion coefficient for the system PMA/copper in pure water and broadening of the distribution ($\Delta G(D)$). The scattering angle is given in the final column

C_p (g ml^{-1})	f	α'	D (cm^2 s^{-1}) $\times 10^{-7}$	$\Delta G(D)$	Angle (deg.)
0.0090	0	0	7.95	0.58	20
	0.125	0	4.86	0.4	20
		0.4	7.65	0.54	20
		0.9	10.6	0.7	20
	0.08	0.05	4.77		30
0.029	0.125	0	3.73	0.32	30
		0.4	8.62	0.44	30
0.041	0	0	4.90	0.55	20

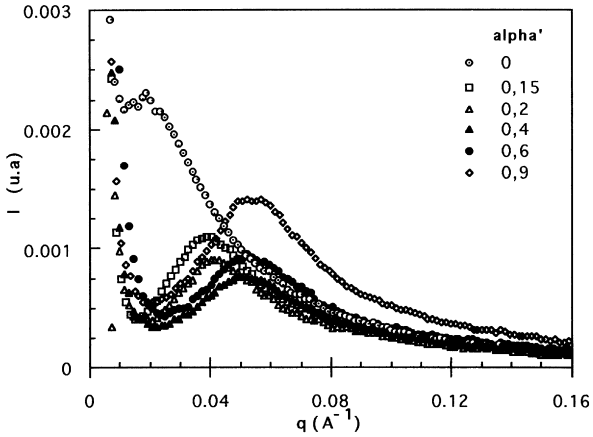

Fig. 8. X-ray scattering curves at different α' values for PMA in pure water; $C_p = 9 \times 10^{-3}$ g ml^{-1}, $C_{pM} = 0.105$ M.

increases as typically observed with polyelectrolytes. Nevertheless, it does not reach a value close to zero when q tends to zero which indicates the presence of heterogeneities in the solutions (Fig. 8).

In the presence of NaCl, the intensity at small q increases with respect to that measured in pure water, which is consistent with the screening out of the electrostatic interactions. Upon α' increasing, its value continuously decreases due to the polyelectrolyte effect and finally for $\alpha'' > 0.4$ a peak can be clearly observed in the scattering functions. In fact the salt concentration used in these experiments is not high enough to screen out the electrostatic repulsions and some correlation between the chain can be observed.

When copper is present in the solutions, the intensity at small q passes through a maximum for $\alpha' = 0.15$ and its value is always much higher than that measured in pure water or in water 0.025 NaCl. From $\alpha' = 0.10$, the curve exhibits a peak which is shifted towards high q values when α' increases. Qualitatively if $\alpha' > 0.6$, the scattering functions look like those observed in the presence of salt.

The effect of nickel ions seems to be intermediate between those of Na and Cu. The observations are summarised in Figs. 12–14 where we have respectively plotted the scattered intensity at $q = 0.005$ Å^{-1}, q_{max} and I_{max} versus α'.

3.3.2. Discussion

3.3.2.1. Small q *range.* At $\alpha' = 0$, the value of the scattered intensity extrapolated at $q = 0$ is the same for the three salts and is consistent with the value which can be calculated from the relation:

$$\frac{1}{C_p M_w} = \frac{BK^2 N_a}{m^2 I} + 2A_2 \qquad (19)$$

where B is the apparatus constant, K^2 is the contrast factor, m the molecular weight of the monomer and A_2 the second virial coefficient. This expression works for neutral

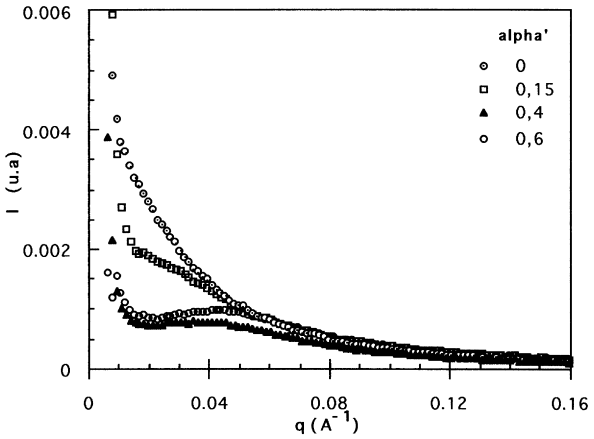

Fig. 9. X-ray scattering curves at different α' values for PMA in the presence of $NaNO_3$ (0.05 M); $C_p = 9 \times 10^{-3}$ g ml^{-1}, $C_{pM} = 0.105$ M.

polymers. B, K^2 and A_2 were obtained from light and X-ray scattering experiments performed on PMA in 0.1 N HCl, on the unionised polymer [8]. This means that in the presence of NaCl, the electrostatic repulsions are completely screened out and with copper and nickel the ion binding lead to the formation of a neutral polymer.

When α' increases, I decreases continuously in the case of $NaNO_3$; this indicates the appearance of the polyelectrolyte effect. The behaviour in the presence of copper is quite different. In the first step of the neutralisation up to $\alpha' = 0.16$, the value for which all the copper ions are bound on the polymer, I increases, which is the inverse effect to that expected. Since our light static and dynamic light scattering experiments did not reveal aggregates, we cannot attribute this behaviour to an intermolecular association. Such an increase of I may be simply explained by a change of the contrast factor due to the ionic complexation. Indeed, the scattering entity is no longer the PMA more or less ionised but a chain which contains a fraction of copper ions. One can calculate the contrast factor for this range of α' by using

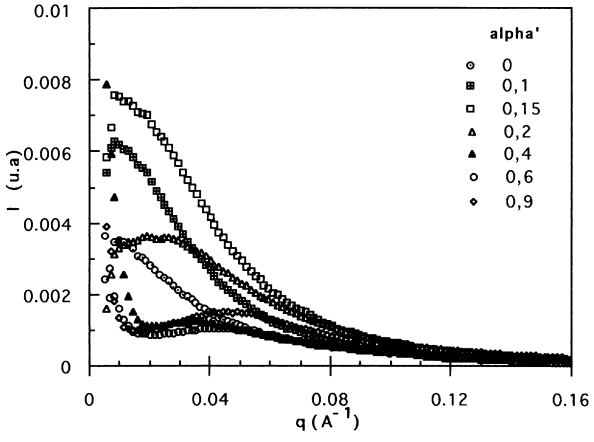

Fig. 10. X-ray scattering curves at different α' values for PMA in the presence of copper ($C_{Cu} = 8.33$ mM); $C_p = 9 \times 10^{-3}$ g ml^{-1}, $C_{pM} = 0.105$ M.

the results of the spectroscopic complexation study [31] which shows that, in a first approximation:

(i) the PMA–copper complex is a binuclear species $(R–COO)_4Cu_2$;

(ii) the concentration of bound copper is $Cui = \alpha' C_{pM}/2$;

(iii) the fraction of ionised carboxylic functions is zero.

Hypothesis (ii) is consistent with the experimental results of Fig. 10 which shows correlation peaks when $\alpha' > 0.2$. We will consider the chain of N monomer units as constituted by:

$(1 - \alpha')N$ unionised monomer units R–COOH with a contrast factor K_1;

no ionised monomer units; $(\alpha'/4)N$ complexes $(R–COO)_4Cu_2$ with a contrast factor K_3.

For the calculation of the scattering length density of the solvent, the counter ions and the added salts are neglected. Finally, the average contrast length is obtained from the simple relation:

$$K = (1 - \alpha')K_1 + \frac{\alpha'}{4}K_3 \tag{20}$$

The different values used in this calculation are given in Table 3. The scattered intensities obtained for $\alpha' = 0.1$ and 0.15 were normalised to this average contrast factor K_2. Fig. 15 shows that the extrapolation of I/K^2 is the same for the three values of α'. This result is consistent with a complete binding of the copper ions according to an intramolecular mechanism without aggregation. The same evaluation was made in the case of nickel, but the normalisation of the scattered intensity by the factor K^2 does not lead to a superimposition of the curves obtained at $\alpha' = 0$ and 0.1. This confirms that Ni^{2+} interacts less strongly with PMA and that a polyelectrolyte effect appears for $\alpha' = 0.10$ due to the presence of ionised carboxylates.

3.3.2.2. Scattering peak. The logarithmic variations of q_{max} versus α' shows that similar data were obtained with Na, Cu and Ni while the values corresponding to pure water are much higher. In previous work we have shown that in pure water this variation exhibits a discontinuity which reflects the conformational change of PMA which passes from a compact to an extended conformation.

The lower value of q_{max} in the presence of copper is expected for a lower ionisation of the polymer. The discrepancy decreases significantly when the abscissa is the true ionisation degree of the polymer calculated taking into account the ion binding, which may indicate that the complexation is the main phenomenon. However, in this analysis we neglect the decrease of the ionic strength due to the complexation while it is known that this must induce an increase of q_{max}, as observed with $NaNO_3$. In fact these antagonistic effects must be taken into account in order to explain the q_{max} shifts. One may consider as a coincidence the similarity of the results obtained with the three salts. The same discussion can be made concerning the I_{max} values.

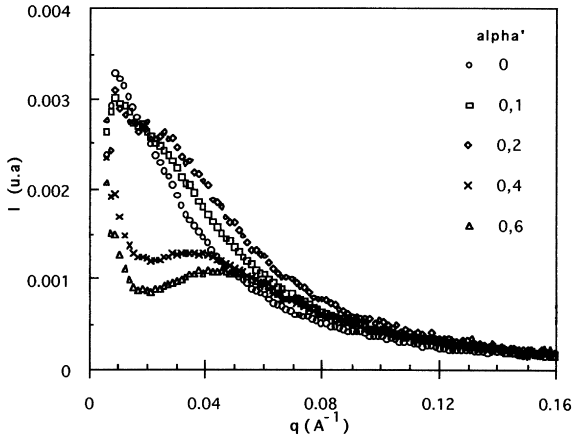

Fig. 11. X-ray scattering curves at different α' values for PMA in the presence of nickel (C_{Ni} = 8.33 mM); $C_p = 9 \times 10^{-3}$ g ml^{-1}, C_{pM} = 0.105 M.

3.3.2.3. Excess of scattered intensity at small q. An excess of scattered intensity at small q was observed for all the solutions in pure water and for the solutions in the presence of $NaNO_3$, $Cu(NO_3)_2$ and $NiSO_4$ for α' higher than 0.15, 0.4 and 0.2 respectively. This indicates the presence of heterogeneities frequently observed in polyelectrolyte solutions and objects of many controversies [40–43]. Generally, it seems that the more charged the polymer, the more important this small q anomaly is. It is interesting to note that in the case of copper for which aggregation was expected, these anomalies appear only at high values of α' when the polyelectrolyte character appears. For Na and Ni the polymer behaves as a polyelectrolyte at lower α' values. The light and X-ray scattering results are then in good agreement and they clearly show that the complexation is mainly an intramolecular phenomenon, at least in the explored concentration range.

3.3.2.4. Chain conformation. In the case of copper, the scattering function does not exhibit correlation peaks at low ionisation and it may be possible to draw some conclusions on the polymer conformation. Values of the radius of gyration equal to 54, 38 and 34 Å for $\alpha' = 0$, 0.10 and 0.15 respectively, can be obtained from the Guinier range. This means that the chain dimensions decrease due to the ion binding. Since no aggregates were observed under these conditions, this confirms an intramolecular process for the cation binding.

Some of the scattering functions are represented in the Kratky representation in Fig. 16. For copper and in the high q range, the scattered intensity varies as q^{-3} and q^{-2} at low and high α' values respectively. The exponent -3 reflects a compactness of the macromolecular coil while -2 corresponds to a quasi-gaussian statistic. Fig. 16 shows that the compactness of the conformation is more pronounced in the presence of copper at $\alpha' = 0.1$ than in HCl 0.1 N. However, a behaviour in q^{-4} indicating a sharp boundary between two

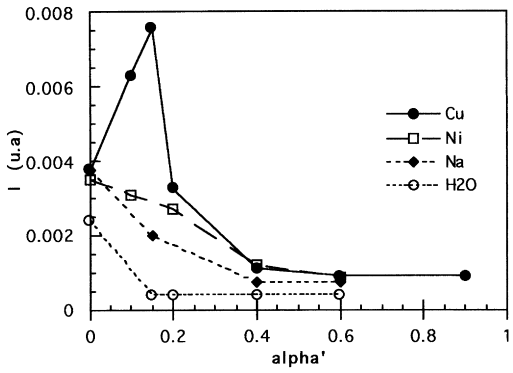

Fig. 12. Variation of the scattered intensity at $q = 0$ versus α' from the experiments of Figs. 8–11.

levels of scattering length density is never observed, meaning that the coil remains partially swollen. In the presence of copper, the variation in q^{-2} is reached for $\alpha' = 0.5$, while it is observed at $\alpha' = 0.1$ and 0 for Ni and Na respectively. This reflects the difference in the interaction strength between the different cations.

These results allow us to clearly differentiate the screening out and complexation effects. The polymer loses its polyelectrolyte character when the complexation constant is very high, as in the case of copper, and recovers it when all the available copper ions are bound. In the case of Ni, the ionisation equilibrium of the carboxylates is not

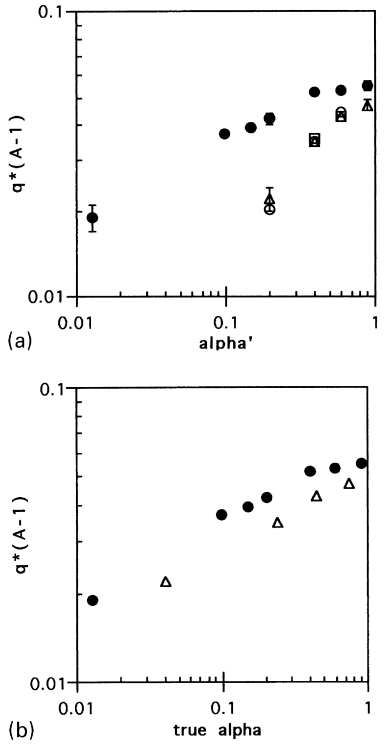

Fig. 13. Variation of the position of the peak maximum from the results of Figs. 8–11. (a) Plotted versus the degree of neutralisation α': pure water (●), in the presence of Na (□), Cu (△), Ni (○). (b) Plotted versus the degree of ionosation: pure water (●), in the presence of Cu (△).

Table 3
Scattering characteristics of the different entities present in the PMA/copper solutions

Elementary diffuser	Number of electrons	Molecular volume ($cm^3\ mol^{-1}$)	ρ (cm^2)	K (cm)
R–COOH	45	59.3	1.29×10^{11}	3.45×10^{-12}
$R–COO^-$	45	37.5	2.04×10^{11}	6.85×10^{-12}
$(R–COO)_4Cu_2$	234	83.7	4.75×10^{11}	2.65×10^{-11}
Cu^{++}	27	− 33.16	1.38×10^{11}	
NO_3^-	30	34.4	9.4×10^{10}	
H_2O	10	18	1.48×10^{11}	

completely shifted, the polymer keeps a polyelectrolyte character in the whole range of α' and the screening effect of the excess ions plays a partial role, while for monovalent cations this latter effect is predominant. The dimensions of the chains neutralised by the complexation are lower than those of the unionised one. Since aggregation is not observed, this strong collapse suggests an intramolecular binding associating two copper atoms with four carboxylates far along the chain (model (d)). Further experiments are necessary to describe definitively the structure of the coil and its evolution when an excess of ionised groups appears along the chain. In order to approach such a description, we have performed some viscosity and fluorescence measurements.

3.4. Viscosity

In Fig. 17 are represented the variations of reduced viscosity η_{red} as a function of α' for PMA ($C_{pM} = 100$ mM) in pure water and in the presence of 1 and 2.5 mM of copper. Three regimes can be identified in these curves: in the lower α' range whose upper limit increases when C_{Cu} increases, η_{red} slightly increases in pure water and remains very low in the presence of copper. In a second range, the η_{red} increases more sharply to reach a constant value in the high α' range. Such behaviour is anomalous with respect to that of other polyelectrolytes for which the variation is monotonous. It is generally attributed to conformational change: at low pH, hydrogen and/or hydrophobic bonds are responsible for a collapsed conformation whose exact structure is not elucidated. At higher pH, the electrostatic repulsions lead to a chain expansion.

In the presence of copper, the value at $\alpha' = 0$ is much lower than that measured in pure water, which is in good agreement with the X-ray experiments. Moreover the shift of the transition suggests that the copper binding maintains this compactness up to the total consummation of copper ions, as already observed by Mandel et al. [28,29]. If this strong collapse of the chain is probably related to the formation of binuclear complexes where groups far along the chain are involved, with creation of loops, one may assume that they are stable only when the chain is neutral but they disappear for a given amount of charged groups at higher pH. A strong expansion should be expected, which is not the case since the reduced viscosity reaches, at $\alpha' = 1$, values

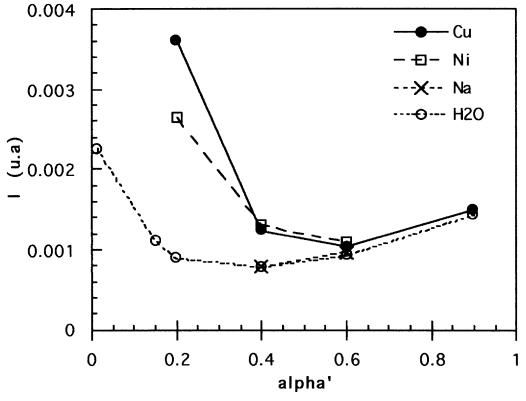

Fig. 14. Variation of the maximum scattered intensity of the peak versus α' from the experiments of Figs. 8–11.

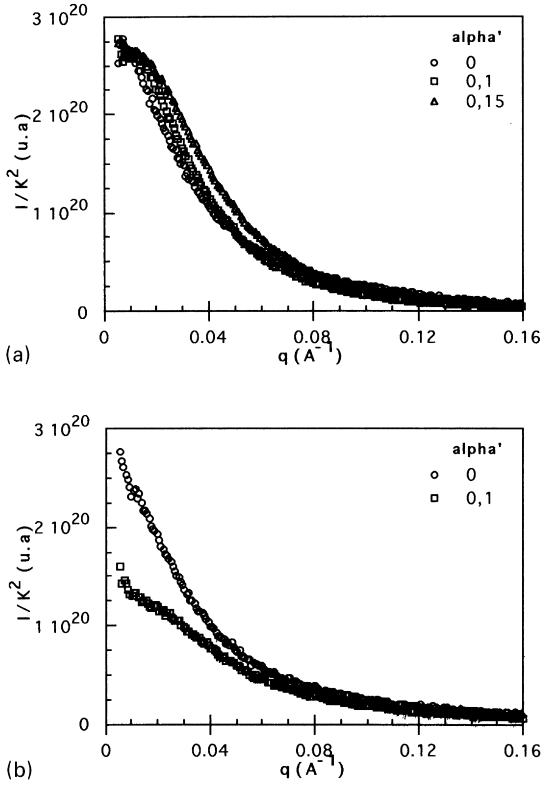

Fig. 15. Variations of the scattered intensity normalised to the contrast factor (see text) for copper (a) and nickel (b) from results of Figs. 10 and 11 respectively.

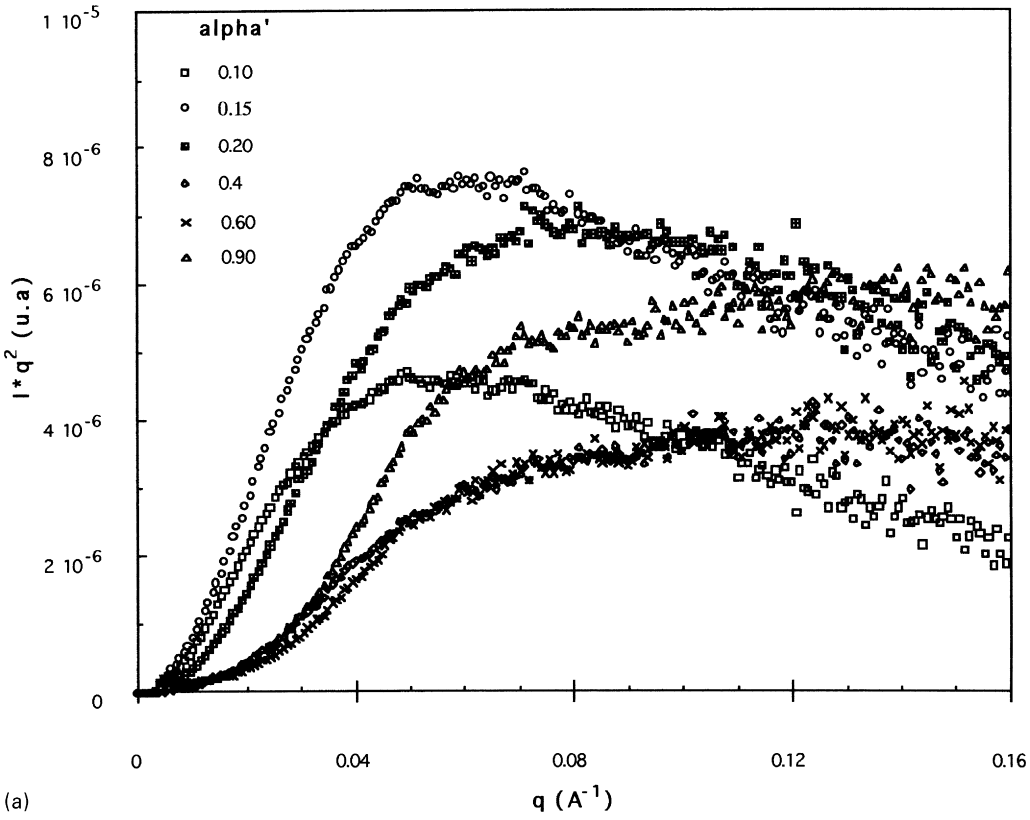

(a)

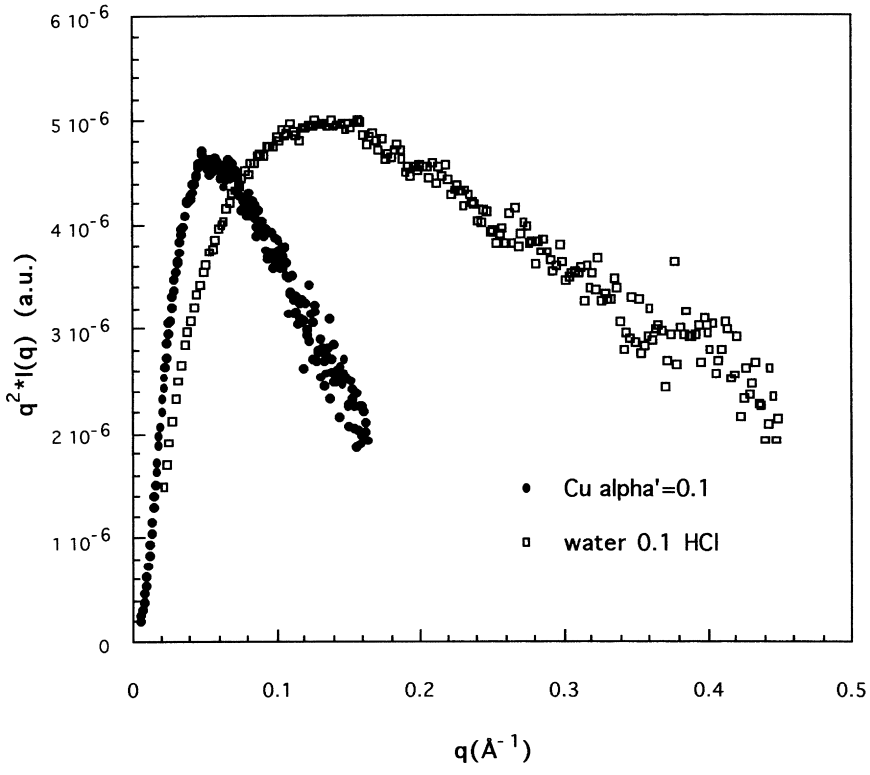

(b)

Fig. 16. Scattering functions in the Kratky representation. (a) PMA–copper for different α' from the results shown in Fig. 10. (b) PMA–copper at $\alpha' = 0.1$ (●) and PMA in water 0.1 M HCl (□).

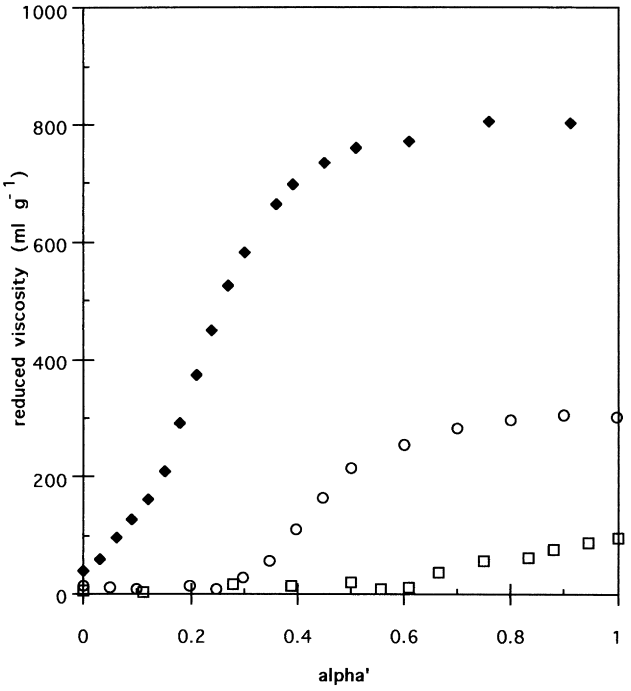

Fig. 17. Variation of the reduced viscosity of PMA ($C_{pM} = 10$ mM) versus α' in the presence of different concentrations of copper, pure water (◆) $C_{Cu} = 1$ mM (○), $C_{Cu} = 2.5$ mM (□).

much lower than in pure water. This also confirms the EPR and u.v.–vis experiments which have shown that the binuclear complexes subsist even at high pH. However, we cannot exclude complexes built from neighbouring carboxylates and assume the existence of a variety of complexes.

3.5. Fluorescence

Fig. 18 shows the variations of I_1/I_3 (the ratio of the intensities of the second to the third peaks of the pyrene emission spectrum) in several conditions: pure water, 0.05 M NaCl and 8 mM $Cu(NO_3)_2$. The superimposition of the three curves is quite remarkable. Other authors have previously used this technique in order to visualise the conformational transition of PMA in water. Our results confirm their observations. The fluorescence behaviour of pyrene in PMA solutions is characterised by a very low value of I_1/I_3 at $\alpha' = 0$ and by an abrupt increase for the $0.1 < \alpha' < 0.25$ range which corresponds exactly to the viscosimetric transition (Fig. 17). For $\alpha' > 0.25$, I_1/I_3 stabilises around 1.9, a value characteristic of a pure water environment for the probe. It is very surprising to observe that the polarity of the compact structure of PMA is much lower than that of micelles of classical surfactants: I_1/I_3 is respectively 1.4, 1.2 and 1.2 for sodium dodecyl sulphate, hexadecyltrimethylammonium or non-ionic surfactants. It is probable that due to the ability of PMA to form helix portions, pyrene molecules find a local environment inside these helices, completely isolated from water. When α' increases, one may suppose that the chain expansion due to the electrostatic repulsion makes free the pyrene molecules which are rejected in the bulk. The results found with Na and Cu do not confirm such an explanation.

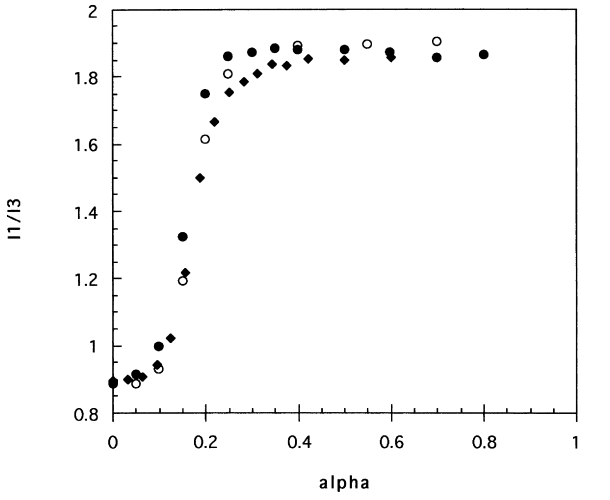

Fig. 18. Variation of the ratio I_1/I_3 versus α', $C_{pM} = 10$ mM, in pure water (○); $C_{Cu} = 1$ mM (●), $C_{NaCl} = 0.05$ M (◆).

It is well known that the viscosity transition of PMA is shifted towards higher values of α' in the presence of NaCl [7]. For this reason, a shift in the I_1/I_3 abrupt increase is also expected, which is not observed in the results shown in Fig. 18. In the case of copper, the structure of PMA at $\alpha' = 0$ is more compact than in water, however, the initial value of I_1/I_3 is exactly the same. Moreover, in our experimental conditions, the conformational transitions as measured by viscosimetry are centred around $\alpha' = 0.4$, while the I_1/I_3 curve is not shifted with respect to those corresponding to pure water and 0.05 M NaCl.

These results are very interesting because they clearly indicate that the pyrene fluorescence does not reflect the overall conformation changes of the macromolecule but very local changes of segment conformation. Moreover, these changes are not directly correlated to the average charge density of the polymer since they appear (in the case of Cu) at α' values where the ionisation is almost zero. One may assume that the hydrogen or hydrophobic bonds which stabilise the compact structure are more sensitive to the thermodynamic quality of the solvent which is modified by addition of NaOH than to changes in the charge density. This may be understood by considering that the electrostatic repulsions are long range interactions and have negligible effects on the local polymer structure. Finally, two transitions may be considered which coincide in the case of pure water: the first one should be very local and the second one should concern the overall macromolecule.

4. Conclusion

Phase diagrams of the system PMA/copper were

constructed. Their characteristics can be interpreted in the terms of a simple thermodynamic model and the solubility limits can be evaluated using the complexation constants already determined in the literature.

The light and X-ray studies indicate that the best model for the PMA chain interacting with copper ions is model D of Fig. 1. In the dilute regime of polymer concentration investigated here, the complexation phenomenon is intramolecular since no aggregation is observed. Due to the chain folding allowing the binuclear complex formation, the structure is much more compact than in pure water. When α' increases, the scattering curves exhibit the characteristics of neutral or charged polymers, before and after the complete copper ions binding, respectively. This confirms the high complexation constant of copper. In the case of Ni of lower constant, the polyelectrolyte effect is always present.

Fluorescence measurements in the presence of NaCl and $Cu(NO_3)_2$ reveal two different transitions: a local conformation change and an abrupt change of the overall dimensions of the coil. The latter has an electrostatic origin which implies long range interactions. The former is more difficult to understand and may be related to simple solvent effects.

Acknowledgements

The authors would like to thank Dr. Ph. Chaumont for preparing the PMA sample for this study and M. Duval for performing dynamic light scattering experiments, at the C. Sadron Institute in Strasbourg. Mrs. Bourgaux is also thanked for her help in the X-ray scattering experiments performed at the LURE laboratory in Orsay.

References

[1] Katchalsky A. J Polym Sci 1951;7:393.
[2] Arnold R, Overbeek JTh. Rec Trav Chim 1950;69:192.
[3] Leyte JC, Mandel M. J Polym Sci 1964;A2:1879.
[4] Liquori AM, Barone G, Crescenzi V, Quadrifoglio F, Vitagliano V. J Macromol Chem 1966;1:291.
[5] Crescenzi V. Adv Polym Sci 1968;5:5388.
[6] Katchalsky A, Eisenberg H. J Polym Sci 1951;6:145.
[7] Heitz C. Thesis, Louis Pasteur University, Strasbourg, France, 1996.
[8] Heitz C, Rawiso M, François J. Polymer, in press.
[9] Armstrong RW, Strauss UP. In: Mark HF, Gaylord NG, Bikales NG, editors. Encyclopedia of polymer science and technology, vol. 10. New York: Wiley-Interscience, 1969:781.
[10] Strauss UP, Ander P. J Am Chem Soc 1958;80:6494.
[11] Strauss UP, Siegel AJ. J Phys Chem 1963;67:2683.
[12] Strauss UP, Leung YP. J Am Chem Soc 1965;87:1476.
[13] Truong ND, Galin JC, François J, Pham QT. Polymer Communication 1984;25:208.
[14] Rahbari R, François J. Polymer 1988;29:845 and 1992;33:1449.
[15] Ikegami A, Imai N. J Polym Sci 1962;56:133.
[16] Flory PJ. J Chem Phys 1953;21:162.
[17] Drifford M, Dalbiez JP. J Phys Lett 1988;46:L–311.
[18] Nierlich M, Boué F, Oberthür R. J Phys France 1985;46:649.
[19] Williams CE, Nierlich M, Cotton JP, Jannink G, Boué F, Daoud M, Farnoux B, Picot C, de Gennes PG, Rinaudo M, Moan M, Wolff C. J Polym Sci, Polym Lett Ed 1979;17:379.
[20] Kaji K, Urakawa H, Kanaya T, Kitamaru R. J Phys France 1988;49:993.
[21] Xiao L, Reed WF. J Chem Phys 1991;94(6):4568.
[22] Boudenne N, François J. Macromol Chem Phys 1995;196:3941.
[23] Förster S, Schmidt M, Antonietti M. Polymer 1990;31:781.
[24] de Gennes PG, Pincus P, Velasco RM, Brochard F. J Phys (Paris) 1976;37:1461.
[25] Odijk T. Macromolécules 1979;12:688.
[26] Pfeuty P. J Phys (Paris) 1978;C2:149.
[27] Borue V, Erukhimovitch I. Macromolecules 1988;21:3240.
[28] Mandel M, Leyte JC. J Pol Sci, part A 1964;2:3771.
[29] Mandel M, Leyte JC. J Pol Sci, part A 1964;2:28831.
[30] Leyte JC, Zuiderweg LH, van Reisen M. J Phys Chem 1968;72:1127.
[31] François J, Heitz C, Metsdagh MM. Polymer, in press.
[32] Zana R. In: Zana R, editor. Surfactant solutions. New methods of investigation, chapter 1. New York: Plenum Press, 1987.
[33] Kalyanasundaran K, Thomas JK. J Am Chem Soc 1977;100:5951.
[34] Libeyre R, Sarazin D, François J. Polym Bull 1981;4:53.
[35] Duval M. Thesis, Louis Pasteur University, Strasbourg, France, 1985.
[36] Olivera de la Cruz M, Belloni L, Delsanti M, Dalbiez JP, Spalla O, Drifford M. J Chem Phys 1995;103:1.
[37] Wittmer J, Johner A, Joanny JF. J Phys (Paris) 1993;11(5):635.
[38] Axelos MAV, Metsdagh MM, François J. Macromolecules 1994;27:6594.
[39] Sedlak M, Konak C, Stepanek P, Jakes J. Polymer 1987;28:873.
[40] Lin SC, Lee WL, Schurr. Biopolymers 1985;17:1041.
[41] Drifford M, Dalbiez JP. J Phys Chem 1984;22:3568.
[42] Nicolai T, Mandel M. Macromolecules 1989;22:2348.
[43] Fulmer AW, Benbasat JA, Bloomfield VA. Biopolymers 1981;30:1147.